

Brownian Dynamics Simulations of Local Motions in Polyisoprene

David B. Adolf and M. D. Ediger*

Department of Chemistry, University of Wisconsin—Madison, Madison, Wisconsin 53706

Received April 11, 1991

ABSTRACT: Brownian dynamics computer simulations have been performed on polyisoprene chains containing 67 repeat units. The simulated trajectories were used to generate three orientational autocorrelation functions analogous to those sensed by ^{13}C NMR T_1 experiments. Agreement between the simulation and dilute-solution NMR experiments is encouraging. Differences in the dynamics of various C-H vectors in the polymer backbone are quantitatively reproduced by the simulation. The simulations indicate the presence of substantial librational motions on a time scale of a few picoseconds. Correlated pairs of transitions occur infrequently. The role of cooperativity in conformational transitions is examined, and a new method of examining cooperativity is presented. For polyisoprene, distortions in atomic positions accompanying a conformational transition are localized to about one repeat unit.

I. Introduction

The local segmental dynamics of polymer chains have an important influence on the macroscopic properties of polymeric systems. These dynamics have been extensively studied with a wide variety of experimental techniques.¹ While these investigations have provided important insights into local polymer dynamics, some critical questions are not directly addressed by experiments. For example, what types of cooperative motion allow conformational transitions to take place in the middle of a polymer chain? Over what length scales are motions cooperative? What role does the potential energy surface play in local polymer dynamics?

Computer simulations provide a means of directly examining the detailed mechanisms of local polymer dynamics. This approach has been previously utilized by Helfand and co-workers,² van Gunsteren,³ Karplus,⁴ Evans,⁵ Fixman,⁶ and others. The simulation of polymers with various structures should significantly further our understanding of structure/property relationships.

In this paper we present Brownian dynamics simulations of the local dynamics of polyisoprene. A preliminary account of this work has been given elsewhere.⁷ This work builds upon Brownian dynamics simulations of polyethylene by Helfand and co-workers.² Polyisoprene was selected for our simulations for two reasons. First, a considerable amount of experimental work on local dynamics in polyisoprene in dilute solution is available for comparison. This is not the case for polyethylene. Second, we wanted to determine if the more heterogeneous (and thus more typical) structure of polyisoprene would lead to qualitatively different dynamics than those observed in the polyethylene simulations.

The insights gained from a computer simulation are applicable to real systems only to the extent that the simulation is realistic. Comparison with experimental observables is thus an important component of our simulation work. In sections III and IV, we compare the polyisoprene simulations to experimental results from ^{13}C NMR. We use the simulation output to generate three orientation autocorrelation functions analogous to those sensed in NMR T_1 experiments. While the agreement is far from perfect, certain aspects of the experimental results are captured very well by the simulations. For example, differences in the dynamics of different C-H vectors within the repeat unit are well reproduced by the simulations. Both the simulations and experiments indicate that the

orientation correlation functions associated with C-H vectors are strongly nonexponential.

The correspondence between experiments and simulations is sufficiently strong to justify a microscopic analysis of the conformational dynamics occurring in the simulation (see section V). These are features that are not directly accessible by experiments. The simulations indicate the presence of substantial librational motions on a time scale of a few picoseconds; this is much faster than the average time between conformational transitions. The role of cooperativity in conformational transitions is discussed, and a new method of examining cooperativity is presented. For polyisoprene, it appears that distortions in atomic positions accompanying a conformational transition are very localized; the length scale for cooperativity is only about one repeat unit. Only a few backbone carbons must move cooperatively to allow a conformational transition to occur. While Helfand et al.² found second-neighbor torsions to be most important in polyethylene, first-neighbor torsions play a more important role in localizing transitions in polyisoprene. Finally, we note some intriguing differences between the correlation times for backbone C-H vectors and the average time between conformational transitions.

II. Simulation Description

Brownian dynamics simulations have been previously utilized by a number of groups to examine the dynamics of long-chain molecules.²⁻⁶ A useful introduction to Brownian dynamics simulations is by comparison to the more familiar molecular dynamics simulations.³ This comparison will help the reader to assess the implications of the approximations utilized within Brownian dynamics simulations. Molecular dynamics simulations use Newton's equation of motion

$$m_i \ddot{\mathbf{a}}_i = \vec{F}_i \quad (1)$$

for a collection of objects with mass m_i . \vec{F}_i represents the sum of all external forces experienced by object i and is related to the gradient of the potential energy U . Given the position and momentum of an object at time t_1 , the position at time t_2 can be determined by numerically integrating eq 1. Performing this operation successively creates the trajectory of the particle as a function of time. In principle, U is a function of the coordinates of all the particles in the simulation. For a study of local polymer motions in dilute solution, this would likely include one

polymer chain (or one section of a chain) and thousands of solvent molecules.

Brownian dynamics simulations utilize the Langevin equation

$$m_i \ddot{a}_i = -m_i \beta_i \dot{v}_i + \bar{F}_i + \bar{N}_i(t) \quad (2)$$

The two new terms (relative to eq 1) describe interactions between the particles of interest and a bath. For our simulations, a section of a polymer chain is the system of interest and the solvent is the bath. The bath damps the motion of the particles with a friction term (of magnitude β_i) and supplies stochastic forces (\bar{N}_i), which mimic the effect of collisions between solvent molecules and the polymer.

For our simulation, we use the high-friction limit of eq 2. For overdamped motions, the inertial term can be ignored. In this case, the equation of motion is given by

$$\dot{v}_i = \frac{-\bar{\nabla}_{r_i} U}{\beta_i m_i} + R_i(t) \quad (3)$$

where

$$\langle \bar{R}_i(t) \bar{R}_k(t') \rangle = \frac{2K_b T}{\beta_i m_i} \delta_{ik} \delta_{tt'} \quad (4)$$

Here K_b is Boltzmann's constant and $\langle \rangle$ represents an ensemble average. The stochastic force term $\bar{R}_i(t)$ contains δ functions indicating that the forces are uncorrelated both spatially and temporally. The average magnitude of the stochastic forces is fixed by the simulation temperature. The potential U is the polymer intramolecular potential. Thus in our simulation the solvent is treated as a viscous, structureless continuum. Equation 3 is the same equation of motion used by Helfand and co-workers to simulate polyethylene.²

The tradeoffs between molecular dynamics and Brownian dynamics are clear. In molecular dynamics, the polymer/solvent interactions are explicitly treated at the cost of a much larger simulation requiring correspondingly more computer time. With Brownian dynamics, the long trajectories required for this study could be obtained with a reasonable amount of computing time (a few hundred hours on an IBM 3090), albeit at the cost of introducing considerable approximations in the treatment of the solvent. The effects of these approximations are discussed in section IV.

Structure. Figure 1 shows the actual structure of *cis*-polyisoprene, along with the structure used in the simulations. Following other workers,²⁻⁵ we employed the united atom approximation and collapsed all hydrogens onto their parent carbons. In this spirit, we also collapsed the fairly rigid $\text{HC}=\text{C}(\text{CH}_3)$ group into one unit. The simulated polymer chain consisted of 67 repeat units (201 beads), each with the geometry shown in Figure 1. Periodic boundary conditions^{2b,8} were used to avoid chain end effects. Thus, the dynamics of the simulated polymer mimic that of a section of an infinitely long chain. The end-to-end distance of the simulated chain was restricted to about 4.3 nm, roughly the average value for a chain with the specified structure and potentials. van der Waals volume increments⁹ and the Stokes-Einstein equation were utilized to generate a suitable coefficient of friction for the $\text{HC}=\text{C}(\text{CH}_3)$ bead relative to the value of 1.40×10^3 kg/ns-mol used for the CH_2 grouping.^{2a} Structural parameters are found in Table IA.

Potential. We utilized a potential that is the sum of three distinct interactions: bond stretching, bond bending, and dihedral (or torsional) angle position. The interactions

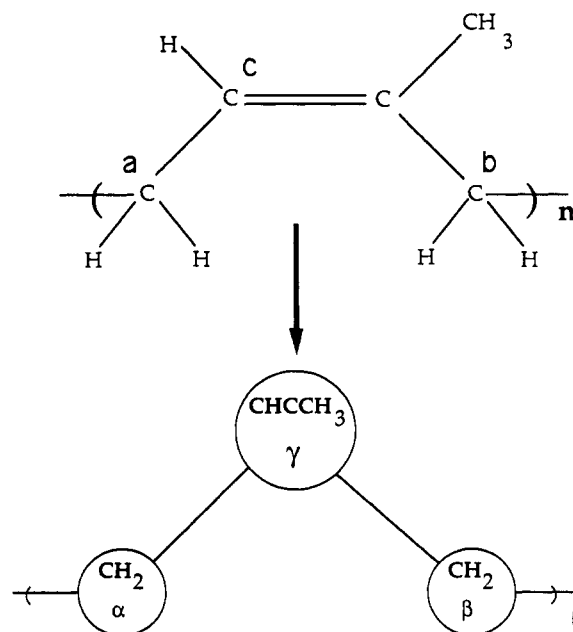


Figure 1. Actual and simulated structure of *cis*-polyisoprene.

Table I
Simulation Parameters and Parameters for the Dihedral Angle Potentials

A. Simulation Parameters			
property	value	property	value
m , kg/mol	α , 0.014	γ_b , kg/part \cdot ns ²	5.81×10^{-17}
	γ , 0.040	γ_θ , J/part	3.02×10^{-19}
	β , 0.014	γ_ϕ , J/part	3.32×10^{-21}
b_0 , nm	$\alpha\gamma$, 0.287	$2K_b T/\beta m$, nm ² /ns (425 K)	α , 5.04
	$\gamma\beta$, 0.287		γ , 3.65
	$\beta\alpha$, 0.154		β , 5.04
θ_0 , deg	$\beta\alpha\gamma$, 109.5		
	$\alpha\gamma\beta$, 120.0		
	$\gamma\beta\alpha$, 109.5		
βm ($=\zeta$), kg/ns-part	α , 2.33×10^{-21}		
	γ , 3.20×10^{-21}		
	β , 2.33×10^{-21}		
B. Parameters for the Dihedral Angle Potentials			
	$\alpha\gamma\beta\alpha$	$\beta\alpha\gamma\beta$	$\gamma\beta\alpha\gamma$
a_0	12.496	10.137	18.567
a_1	-0.350	-0.102	-21.028
a_2	22.253	17.215	-6.354
a_3	-19.233	-19.625	27.280
a_4	-9.3428	-6.534	7.451
a_5	15.562	11.381	3.351

that comprise the potential experienced by bead i are described by the following equations:

$$U_i = \sum_{b(i), \theta(i), \phi(i)} (U_b + U_\theta + U_\phi) \quad (5)$$

$$U_b = 0.5\gamma_b(b_i - b_0)^2 \quad (5a)$$

$$U_\theta = 0.5\gamma_\theta(\cos \theta_i - \cos \theta_0)^2 \quad (5b)$$

$$U_\phi = \gamma_\phi \sum_{n=0}^5 a_n \cos^n \phi_i \quad (5c)$$

The potential experienced by bead i is equal to the sum of three separate potentials over all the bonds, valence angles, and dihedral angles that incorporate bead i . Note that the potential does not include direct interactions between particles more than three positions apart along

Table II
 P_1 Correlation Times (ps) for Polyethylene (425 K)

vector	P_1 correlation times		vector	P_1 correlation times	
	ref 2 ^a	this work		ref 2 ^a	this work
bond	45	43	chord	748	794
bisector	42	48	out-of-plane	516	542

^a Calculated from reported fit parameters.

the chain. Particles farther apart than this along the contour can move through each other (phantom chain approximation). A listing of all the potential parameters for polyisoprene can be found in parts A and B of Table I.

Equations 5a and 5b indicate that the bond lengths and bond angles are harmonically constrained. The reference values for the harmonic constraints are chosen realistically. Following ref 2, the force constants used for bond stretching and valence angle bending are chosen approximately 3 times looser than realistic force constants to allow for larger time steps of integration. One run has been performed with stiffer values of γ_b and γ_θ (3 times larger than those in Table IA). The simulation with larger values of γ_b and γ_θ showed dynamics only 20% slower than a comparable run with the normal values, and the relative time scales of various polymer motions were the same within statistical error (see below).

The dihedral angle potentials for polyisoprene were generated by performing MM2 molecular mechanics¹⁰ on three small molecules resembling pieces of *cis*-polyisoprene: 2-methyl-2-pentene(3,4), 3-methyl-2-pentene(3,4), and 3-methyl-2-hexene(4,5). The two numbers in parentheses indicate the carbons that form the dihedral angle of interest. A block-diagonalized Newton-Raphson method was used to minimize the overall energy of each molecule at fixed dihedral angle values. Fitting the energy to a fifth-order polynomial produced the a_n terms that appear in eq 5c for the dihedral potential. Three different sets of a_n 's apply to the three different dihedral potentials utilized in our polyisoprene simulations. Two of the potentials are 2-fold ($\alpha\gamma$ and $\gamma\beta$), while the $\beta\alpha$ potential is 3-fold and very similar to the dihedral potential for butane. The conformations shown in Figure 1 define $\phi = 0^\circ$ for the 2-fold potentials, while $\phi = 180^\circ$ for the trans state of the 3-fold potential. Note that potentials for the three dihedral angles are treated independently. Also note that, even though the simulated structure does not contain explicit hydrogens, the potentials were generated from molecules with hydrogens present.

Algorithm. A numerical method developed by Helfand and Greenside¹¹ was used to integrate the equation of motion to second order. Time steps of 5 fs were used for most simulations. Each 1 ns of the simulation trajectory required about 1 h of CPU time on an IBM 3090 with a vector processor. A typical simulation length was 10–20 ns.

To initialize the simulation, a random-coil structure was created. An artificial harmonic constraint was imposed on the chain to force it to acquire the desired distance of 4.3 nm for the periodic boundary conditions previously discussed. The simulation was then performed for 200–500 time steps so that the periodic boundary condition distance would gently assume the required value. This final distance was then used throughout the simulation to locate the periodic boundary beads from the beads at the chain's ends.⁸

As a check we simulated both butane and polyethylene at 425 K and compared our results to those generated by Helfand et al.^{2a} Our transition rate for the one dihedral angle in butane was $65 \pm 2 \text{ ns}^{-1}$ and compared favorably

to that given in ref 2a (67 ns^{-1}). We compared polyethylene results in the form of the autocorrelation functions used by Weber and Helfand.^{2b} The agreement was quantitative. Table II shows the comparison in terms of correlation times. The correlation time, τ_c , is the integral of the correlation function:

$$\tau_c = \int_0^\infty CF(t) dt \quad (6)$$

Here $CF(t)$ denotes a correlation function. Table II reveals that the agreement between our polyethylene simulations and those of ref 2 is excellent. Details on the construction of correlation functions can be found in a previous publication.⁷

III. Correlation Functions: Comparison to NMR Experiments

One major focus of our simulation work is the comparison with experiments. In this section, we compare the simulation results with ^{13}C NMR T_1 measurements of the local dynamics of polyisoprene.¹² Section IV will discuss the quality of the comparison and possible reasons for discrepancies.

NMR Measurements of the Local Dynamics in Polyisoprene. ^{13}C NMR T_1 measurements are sensitive to the reorientation of C–H bonds. The T_1 value depends upon the decay of the P_2 orientation autocorrelation function:

$$CF(t) = \langle P_2(\hat{x}(0) \cdot \hat{x}(t)) \rangle = 0.5 \langle 3(\hat{x}(0) \cdot \hat{x}(t))^2 - 1 \rangle \quad (7)$$

Here P_2 is the second Legendre polynomial and $\hat{x}(t)$ is a unit vector in the direction of a particular C–H bond vector at time t . In general, it is difficult to extract the shape of $CF(t)$ from NMR measurements. However, in the extreme narrowing regime, there is an unambiguous relationship between T_1 and the correlation time τ_c .

$$1/T_1 = K n \tau_c \quad (8)$$

τ_c is the integral of the correlation function (see eq 6). K is a function of the C–H bond length and fundamental constants. A value of $2.29 \times 10^9 \text{ s}^{-2}$ has been determined for $\text{C}_\alpha\text{--H}$ and $\text{C}_\beta\text{--H}$ while for $\text{C}_\gamma\text{--H}$ equals $2.42 \times 10^9 \text{ s}^{-2}$.¹³ Equation 8 is valid when the major mechanism for magnetic relaxation is dipole–dipole interactions between a ^{13}C nucleus and its n -bonded protons. This is the case for polyisoprene. This relationship holds for any type of motion and any correlation function shape as long as the following condition of the extreme narrowing limit applies:

$$(\omega_H + \omega_C)\tau \ll 1 \quad (9)$$

Here ω_H and ω_C are the respective Larmor frequencies for ^1H and ^{13}C NMR and τ represents any time constant that contributes to the correlation function decay.¹⁴

Glowinski et al.¹² have studied the local dynamics of polyisoprene (about 75% *cis*) under extreme narrowing conditions in 10 solvents. Correlation times were determined for carbons a–c in Figure 1. An important general feature of their results is that τ_c depends only on the solvent viscosity and not the solvent identity. The τ_c 's from this experimental study will be compared to the simulation results.

Simulation Correlation Times. In order to facilitate comparison to the NMR results, we used the following procedure. First, vectors with the orientation of the C–H vectors for carbons a–c were constructed with respect to the simulated structure.⁷ Second, correlation functions were calculated for each of these vectors, averaging over all monomer units in the chain. Finally, the correlation

Table III
 P_1 and P_2 Correlation Times (ps) for C-H Vectors:
Simulation and Experiment

T, K	C-H vector	$\tau_c(P_1)$	$\tau_c(P_2)$	$\tau_c(P_2, \text{NMR})^a$
425 (run 1)	C _c -H	200.0	32.3	
	C _b -H	79.4	25.3	
	C _a -H	77.9	21.8	
425 (run 2)	C _c -H	211.9	35.3	
	C _b -H	84.2	27.8	
	C _a -H	76.5	22.6	
330	C _c -H	246.6	64.7	50
	C _b -H	160.5	54.9	40
	C _a -H	151.6	45.0	34
273	C _c -H	417.1	106.5	135
	C _b -H	295.5	92.5	108
	C _a -H	276.1	81.2	92

^a Reference 12.

functions were integrated to yield τ_C . This integration was performed both by direct numerical integration and by analytical integration of the fit to a sum of exponentials (obtained from Provencher's numerical inverse Laplace transform routine SPLMOD).¹⁵ Good agreement was obtained between the two methods.

Table III gives the simulated τ_C values obtained by this procedure. We estimate the accuracy of the P_2 τ_C values to be about 10%, based on the two different runs at 425 K. The errors on the P_1 τ_C values may be somewhat larger, since the decay times were a larger fraction of the trajectory length. Also shown are τ_C values for the NMR measurements with a sample viscosity of 1.6 cP (see below). Only τ_C values for the P_2 correlation function are measured by the NMR experiments. τ_C values for the P_1 correlation function were calculated for comparison.

Breakdown of nT_1 Rule. Equation 8 indicates that different backbone carbons should have about the same values of nT_1 if the associated C-H vectors all have the same τ_C 's (because K is approximately the same for all carbons). The expectation that this should be the case is sometimes referred to as the nT_1 rule. For polyisoprene, nT_1 values for carbons a-c are significantly different. This implies that the correlation times for these vectors are significantly different.^{12,16} It is observed experimentally that the C_c-H vector has the longest τ_C and that C_a-H has the shortest. Furthermore, the experiments show that ratios of these correlation times are independent of temperature and solvent.

Figure 2 shows simulated correlation functions at 425 K corresponding to C-H vectors attached to carbons a-c. The simulated correlation functions decay at different rates and are ordered in agreement with the experimental results. Table IV shows ratios of the correlation times for the various C-H vectors obtained from both simulation and experiment (superscripts indicate different C-H vectors). The ratios of τ_C values from the simulation are roughly independent of temperature, as observed in the NMR experiments. The ratios reported for the NMR experiments are an average over 10 solvents and the temperature range indicated. The ratios from the simulation are in quantitative agreement with the experimental results. The simulation performed with more realistic force constants for bending and stretching also yields ratios of τ_C values in good agreement with experiment.

The breakdown of the nT_1 rule in polyisoprene has sometimes been ascribed to relaxation of the methine carbon with nonbonded protons.¹⁷ Glowinkowski et al.¹² and Gisser et al.¹³ have argued that this is unlikely and that the different values of nT_1 observed for different backbone carbons should be interpreted as different correlation times. The good agreement shown in Table

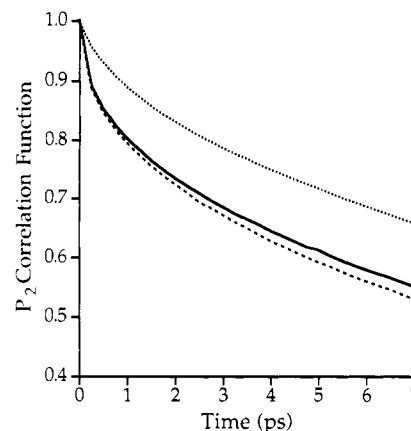


Figure 2. Simulated P_2 autocorrelation functions associated with ^{13}C NMR measurements. The curves show correlation functions for C-H vectors on carbon c (\cdots), carbon b ($—$), and carbon a ($- -$). NMR experiments indicate that the correlation function decay is fastest for C_a-H and slowest for C_c-H in good agreement with the displayed curves. The simulation temperature was 425 K.

Table IV
Ratios of P_2 Correlation Times for C-H Vectors Sensed in NMR Experiment^a

	T, K	τ_c^c/τ_c^a	τ_c^b/τ_c^a
$P_2(\text{simulation})$	425	1.49	1.20
$P_2(\text{simulation})$	330	1.43	1.22
$P_2(\text{simulation})$	273	1.31	1.13
simulation av		1.41	1.18
simulation (425 K, stiff γ_θ and γ_δ)		1.54	1.27
NMR (270–350 K) ^b		1.47	1.18

^a All values are ± 0.10 . ^b Reference 12.

IV between NMR results and the simulations is another indication that the violation of the nT_1 rule is dynamical in nature.

Activation Energies. Activation energies can be calculated from the simulation τ_C values reported in Table III. We have done this for the P_2 correlation times measured in the NMR experiment (see Figure 7). All three C-H vectors yield the same activation energy within statistical error: 7.9 ± 0.5 kJ/mol. This value represents some effective potential barrier height. The NMR experiments also indicate that the three C-H vectors have the same activation energies. However, the observed value of 13 ± 2 kJ/mol (corrected for the viscous flow contribution) does not agree quantitatively with the value from the simulations.

In the case of polyethylene simulations by Helfand and co-workers,² it was observed that the activation energy extracted from the simulations was in quantitative agreement with the barrier height of the input potential. This barrier height corresponded to a trans to gauche conformational change. In the case of polyisoprene, the input potentials contain many barrier heights because three different torsional potentials are utilized. Thus a comparison between the observed activation energy and the input potentials is not straightforward. The barrier heights for the three input potentials are as follows: $\alpha\gamma$, 2 and 18 kJ/mol; $\gamma\beta$, 9 and 17 kJ/mol; $\beta\alpha$, 13, 14, and 19 kJ/mol. The observed activation energy is between the largest and smallest barriers.

Absolute Correlation Times. The comparison of absolute correlation times requires a relationship between the solvent viscosity and the friction coefficient used in the simulation. This is a difficult matter for this system. Since the simulations are performed in the high-friction

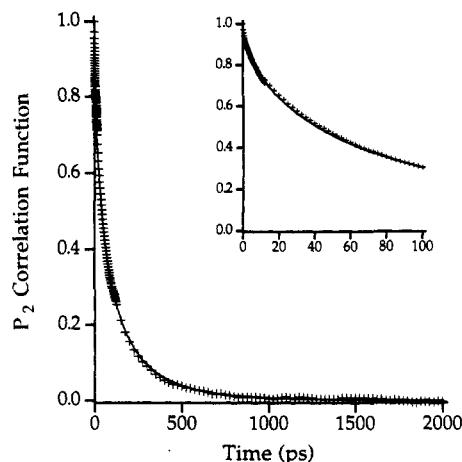


Figure 3. Williams-Watts fit (solid line) of the simulated P_2 autocorrelation function for the C_c -H vector ($T = 273$ K).

limit, τ_C values from the simulation scale linearly with the friction. Glowinkowski et al.¹² have shown that τ_C values from NMR measurements on polyisoprene in dilute solution depend only on the solvent viscosity but have an $\eta^{0.41}$ dependence. A linear relationship between the friction and the viscosity (such as Stokes' law) is not consistent with these assumptions and observations.

One explanation for the unusual viscosity scaling observed in the NMR experiments is that the friction should be regarded as frequency dependent. It has been argued that this has a small effect on τ_C values for low-viscosity solvents (relative to the τ_C expected on the basis of Stokes' law).¹⁸ Thus, for a rough comparison of the experiments and the simulations, we use Stokes' law and a small viscosity. Paul and Mazo¹⁹ have shown that the translational diffusion of alkanes can be explained with Stokes' law using 0.77 Å for the hydrodynamic radius of a CH_2 grouping. This implies that the simulated system has a viscosity of 1.6 cP.

Table III contains both experimental and simulation values of $P_2 \tau_C$ for two temperatures. The experimental values shown in Table III are those appropriate for a solvent with a viscosity of 1.6 cP at the indicated temperatures. Given the factors discussed above, this comparison serves merely to indicate that the τ_C 's from the simulation are reasonably close to experimental values.

Correlation Function Shapes. In recent years there has been considerable interest in the shape of the orientation autocorrelation functions associated with local segmental motions.^{1,20} These shapes contain information about the detailed mechanisms of the local dynamics. We have fit the P_2 correlation functions constructed from the simulation trajectories to the Williams-Watts function:

$$CF(t) = \exp^{-(t/\tau)^\beta} \quad (10)$$

The exponent β indicates the deviation from a single-exponential decay. The Williams-Watts function was chosen as the fitting function because it is an extremely flexible two-parameter function which adequately fits the simulation results. We do not believe the fitting parameters have any fundamental significance for this system.

Figure 3 shows the P_2 correlation function for the C_c -H vector at 273 K fit with the Williams-Watts function. Typically, the fits match the computed correlation functions within 0.02 throughout the decay. In Table V, fits to the P_2 correlation functions associated with C-H bonds in the polyisoprene backbone are presented. For all vectors, the β increases slightly with temperature. The β values for the C-H vectors attached to methylene groups

Table V
Fits to P_2 Correlation Functions to Williams-Watts

T , K	C-H vector	τ , ps	β
425 (run 1)	C_c -H	24.7	0.690
	C_b -H	16.7	0.585
	C_a -H	14.8	0.588
425 (run 2)	C_c -H	25.8	0.684
	C_b -H	17.2	0.572
	C_a -H	14.9	0.585
330	C_c -H	47.8	0.635
	C_b -H	35.2	0.554
	C_a -H	30.2	0.569
273	C_c -H	74.5	0.614
	C_b -H	61.7	0.545
	C_a -H	51.5	0.540

are essentially identical. The β values for the methine vector are somewhat larger.

NMR experiments in the extreme narrowing regime given no information about the shape of the correlation function. Recent NMR measurements by Gisser et al.¹³ through the T_1 minimum have elucidated the general features of the correlation function decay for a dilute solution of polyisoprene in toluene. Motion of the C-H vector occurs on two well-separated time scales. The faster motions (<2 ps) are likely librational motions in dihedral angle potential wells. The slower motions (15 ps to 1 ns, depending on temperature) presumably reflect conformational transitions. Each type of motion accounts for roughly half of the correlation function decay.

The simulations agree with experiments to the extent that strongly nonexponential functions are observed. The experiments indicate a stronger separation of time scales between fast and slow motions than does the simulation.

IV. Discussion of Simulation vs Experiment

The previous section indicates that the simulations match the experimental results in at least two important ways. First, they do a remarkable job of quantitatively reproducing interesting differences in the dynamics of various C-H vectors within the repeat unit. Second, the simulations are designed so that the only solvent-dependent parameter is the friction; the possibility of specific interactions between the polymer and the solvent is ignored. Experiments support this approach, as the observed dynamics depend only on the solvent viscosity and not on the solvent identity. For example, NMR τ_C 's for polyisoprene in hexadecane and *cis*-decalin are nearly identical.¹² These two solvents have significantly different structures and sizes but are essentially isoviscous.

The simulations do not match experimental results in three areas. Most importantly, the experimental τ_C 's scale as $\eta^{0.41}$ while in the simulations τ_C scale with the first power of the friction. Only the ad hoc postulate that the friction scales as $\eta^{0.41}$ can strictly reconcile these results. This is unsatisfactory, as it is known that friction scales as η^1 for large-scale chain motions.²¹ In addition, the activation energy from the simulation is smaller than the experimental value, and the correlation function decay does not occur on two well-separated time scales as experiments indicate.

The differences between the simulations and the experiments arise from the following approximations made in simulations. (1) The structure of the chain has been significantly simplified. Up to six atoms have been collapsed onto a point mass with the friction chosen to mimic that of the group. (2) Independent dihedral potentials and the phantom chain approximation have been used. Unrealistically loose stretching and bending potentials have been utilized. (3) The high-friction

Langevin equation has been used as the equation of motion. Inertial terms have been ignored, and the solvent has been treated as a viscous continuum. The lack of temporal correlation in the stochastic forces ensures that the friction opposing chain motion is the zero-frequency friction (directly proportional to the viscosity).

The use of the high-friction Langevin equation is responsible for the fact that the simulation is inconsistent with the sublinear viscosity dependence observed experimentally. It can be shown that the neglect of the inertial term is not the reason for this discrepancy.¹² Use of colored noise (time-correlated stochastic forces) in the simulation might improve the comparison. Memory functions have been utilized to obtain a frequency-dependent friction coefficient.²² The high-friction Langevin equation will also damp very high frequency motions (such as librations) to an unrealistic extent. This may explain why the experimental correlation function decay occurs on two well-separated time scales, while this is not the case for the simulated decays.

The low value of the activation energy extracted from the simulation may be due to the use of independent dihedral potentials. The optimized one-dimensional potentials used in the simulations might lead to an artificially low barrier compared to motion about an actual dihedral bond where the neighboring dihedral angles will not be in the optimal position. Two-dimensional interdependent dihedral potentials could be efficiently implemented in this type of simulation. It is likely that some part of the error in the activation energy is due to the use of a gas-phase potential instead of a potential of mean force.

V. Microscopic View

Several important features of the experimental results are reproduced by the computer simulations. In particular, the simulation correctly predicts the relative correlation times for different C-H vectors within the repeat unit. Certainly some features of the simulation are not realistic. The sublinear viscosity dependence of the experimental τ_C 's is not consistent with the structure of the simulation. However, given that the simulation correctly predicts relative correlation times, it is reasonable to expect that mechanisms of the local dynamics portrayed by the simulation are at least qualitatively correct. With this assumption, we proceed to analyze those features of the simulated dynamics that are not directly accessible to experiments. Our goal is to extract qualitative features that may help to develop a conceptual picture of the local dynamics in this system.

Librational Analysis. NMR studies of polyisoprene and other polymers have suggested that motions much faster than τ_C play a significant role in the local dynamics.^{13,16} It has been suggested that these fast dynamics occur on the time scale of a few picoseconds and arise from motion within dihedral potential wells. Usually it is presumed that motion within the dihedral angle potential well would account for the fast motions without conformational transitions occurring. We have examined this point with the simulation trajectories by observing how dihedral angles evolve in time. Let a given dihedral angle at an arbitrary starting time be represented by $\phi(0)$. From the trajectory we build a histogram indicating the probability that at time t the dihedral angle will have changed by $|\phi(t) - \phi(0)|$. This quantity is denoted $P(|\phi(t) - \phi(0)|)$ after averaging over all dihedral angles and starting times.

Figure 4 illustrates the dihedral angle distribution for different values of time for the $\gamma\beta$ dihedral angle. Within

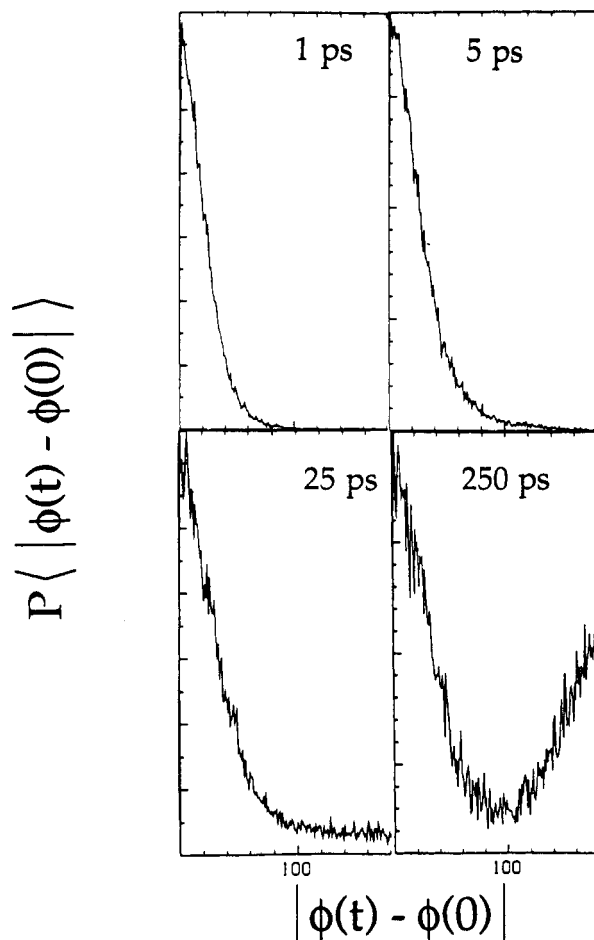


Figure 4. Evolution of the distribution of dihedral angles for the $\gamma\beta$ bond. Motions with a fwhm of 50° take place in less than 1 ps from an arbitrary starting time. Conformational transitions begin to build in at longer times.

one ps, the dihedral angles have already spread into a cone with a fwhm of 50° . This feature of the dihedral angle distribution changes little as time evolves. With increasing time a new peak centered at 180° grows, indicating transitions to the other conformational state. The two features shown in Figure 4 indicate dynamics on two very different time scales. Fast motions within potential wells reach their equilibrium distribution before a significant number of conformational transitions occur. This is consistent with the experimental inferences about librations. Based on the discussion of correlation function shapes in section III, we would expect that the separation of time scales shown in Figure 4 is even more striking in reality. Analogous plots for the two other dihedral angles show qualitatively similar behavior.

Cooperative Transitions. It has long been recognized that individual conformational transitions cannot occur in the middle of a polymer chain if other degrees of freedom do not cooperate.²³ A significant portion of the chain would have to swing rigidly in order for this to occur. The friction associated with this type of motion would be enormous. If this were the normal pathway for conformational transitions, they could not occur on the nanosecond/picosecond time scale and would not be independent of molecular weight. Somehow other degrees of freedom must cooperate with the rotating bond in order to localize the portion of the chain that is required to move. Early proposals for this type of motion suggested crankshaft motions, whereby two nearby, collinear bonds would rotate simultaneously.²⁴ Less restrictive motions have also been proposed, including the "cranklike" motions proposed by

Helfand²³ in which motions occur about two parallel but noncollinear bonds.

Helfand and co-workers² have analyzed Brownian dynamics simulations of polyethylene in terms of cooperative transitions. This analysis requires (a) a definition of a "transition" and (b) a time cutoff that establishes the maximum time between two events which still allows them to be considered cooperative. They utilized curvature in the hazard plot of first-passage times to identify the cutoff time. A transition was defined as the change of a torsional angle from the minimum of one potential well to the minimum of an adjacent well.

Reference 2 reports that 29% of all polyethylene transitions were cooperative by this definition at 425 K. Three bond sequences with the center conformation unchanged were considered. Most of these cooperative transitions were cranklike as Helfand²³ had proposed earlier: 13% of all transitions were gauche migrations and 10% were gauche pair productions. As a test of our procedures, we repeated the analysis of ref 2 on our own polyethylene trajectories. We found 28% cooperative transitions (13% gauche migrations, 10% gauche pair productions) at 425 K, in good agreement with the results of ref 2.

We repeated this procedure on the polyisoprene trajectories. The same definition of a transition was used. A cutoff time of 3 ps at 425 K was derived from the curvature in the hazard plots. The hazard plots were less noticeably curved for polyisoprene than for polyethylene. Cooperative transitions were examined for first- and second-neighbor bonds along the chain. A total of 7% of the transitions were cooperative when the search was restricted to three-bond sequences where the conformation of the center bond remained unchanged. An additional 13% of the transitions were cooperative if first-neighbor cooperativity was also considered. A detailed analysis of the cooperative sequences indicates that any one type of transition accounts for no more than a few percent of the total transitions. This is perhaps not surprising given the heterogeneity of the polyisoprene backbone (a mixture of 2- and 3-fold potentials) in comparison to the polyethylene backbone.

Another View of Cooperativity. The fact that more than two-thirds of all transitions for both polyethylene and polyisoprene occur as isolated transitions requires some additional discussion. How do local conformational transitions occur, if not in cooperative transition pairs? Hall and Helfand have sketched the general outlines of the answer.²⁰ Other degrees of freedom must cooperate with a single conformational transition to localize the distortion of atomic positions. To the extent that neighboring torsions contribute to this process, it must be the case that they usually do not undergo a conformational transition.

A key question is the length scale over which conformational transitions are localized. Does an atom separated by five repeat units from an "isolated" transition adjust its position to relieve the stress created by that transition? It is also interesting to investigate how different degrees of freedom (torsions, bends, and stretches) contribute to the localization and how fast distortions in these coordinates relax.

We have devised a technique for analyzing the trajectory in order to address these issues about distortions accompanying conformational transitions. Conceptually, we take a snapshot of the atomic (or bead) positions on a section of a chain just before and just after a conformational transition. By averaging over thousands of transitions,

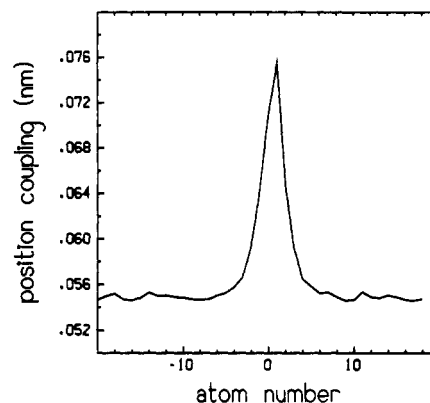


Figure 5. Distortion of atomic positions accompanying a conformational transition in simulated polyisoprene (expression 11). The conformational transition occurs between atoms 0 and 1. The distortion is limited to a few repeat units.

we can determine the average atomic displacements accompanying a conformational transition. Mathematically, we calculate the quantity

$$\langle |\bar{r}_i(t=\tau_{\text{trans}}+\Delta t) - \bar{r}_i(t=\tau_{\text{trans}}-\Delta t)| \rangle \quad (11)$$

Here \bar{r}_i represents the coordinates of the i th atom along the chain. The index " i " is the position of an atom along the chain contour relative to the position of the transforming bond. Typically we calculate the quantity shown for $i = -20$ to $+20$; i.e., we analyze the movements of 20 atoms on each side of the transforming bond. The ensemble average is taken over all transitions occurring in the trajectory. Generally Δt is chosen to be between 0.5 to 10 ps; this is much shorter than the average time between transitions (160 ps at 425 K). Some discussion of the transition time τ_{trans} is required. We used Helfand's definition of a transition (see above) to determine where transitions occurred. However, τ_{trans} was defined to be the last time the potential barrier was crossed before the transforming bond reached the minimum of the second potential well. On the average, τ_{trans} occurred about 5 ps before the minimum of the second well was reached (at 425 K).

Figure 5 shows a plot of expression 11 for polyisoprene at 425 K ($\Delta t = 0.5$ ps). As expected, the two atoms that define the transforming bond show the greatest change in position during the time interval about τ_{trans} . The atomic position distortion drops off quickly as atoms farther from the transforming bond are considered. Six atoms away along the chain contour the displacement is no greater than 20 atoms away. This base line simply reflects thermal motions which occur in any 1-ps interval regardless of whether a transition has occurred nearby. The fwhm of the peak is about three atoms or one repeat unit. This length is a good candidate for the length scale of cooperativity for conformational transitions in polyisoprene.

An analysis similar to expression 11 can be carried out for any degree of freedom in the simulation. We have analyzed coupling with neighboring torsions ϕ_i using the expression

$$\langle |\phi_i(t=\tau_{\text{trans}}+\Delta t) - \phi_i(t=\tau_{\text{trans}}-\Delta t)| \rangle \quad (12)$$

We have also analyzed bond angles and bond stretching with similar expressions. Figure 6 shows the torsional and bond angle coupling at 425 K with $\Delta t = 0.5$ ps for the polyisoprene simulation. Both show maximum distortions at the position of the conformational transition and that the distortion is negligible more than six atoms away from the transforming bond. Thus Figures 5 and 6 show a

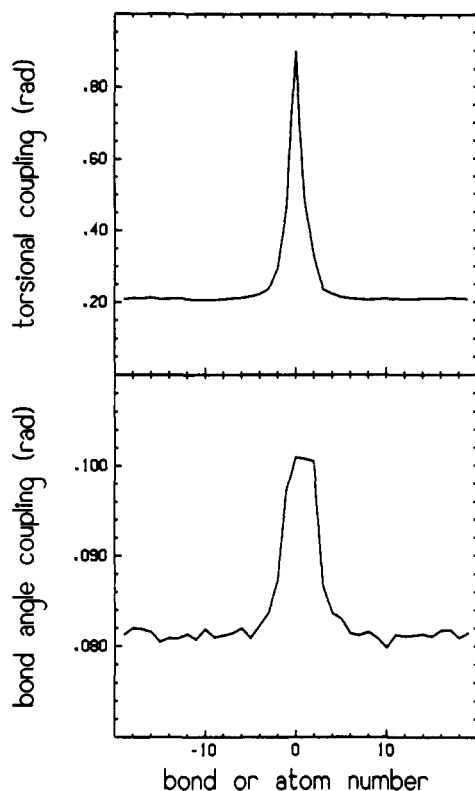


Figure 6. Distortions of torsional modes (top panel) and bond angles (bottom panel) accompanying a conformational transition in simulated polyisoprene. These plots were created from expression 12 and its analogue for bond angles. For the torsional modes, the transition occurs at bond 0; for the bond angles the transition occurs between atoms 0 and 1. The distortions are limited to a few repeat units.

consistent picture of conformational transitions localized to less than two repeat units.

The torsional coupling in Figure 6 is strong for first neighbors but much less important for second neighbors. This is in contrast to the behavior of polyethylene inferred by Helfand et al.² from a hazard analysis. In this latter case, second-neighbor coupling was much more important than first-neighbor coupling. When our polyethylene trajectories are analyzed with expression 12, we also find second-neighbor coupling much more important than first neighbors.²⁵ Presumably the difference between polyethylene and polyisoprene is due to the different structures and potentials of these materials.

We have also investigated different values of Δt in expression 11 and its analogues. The effects on the position and torsional coupling are relatively small; the magnitude and width of the distortion change by less than a factor of 2. For bond angle coupling, the magnitude of the distortion decreases 1 order of magnitude as Δt is increased from 0.5 to 5 ps. This rapid relaxation is presumably due to the stiffness of the bending coordinate. No coupling between the conformational transition and bond stretching (the stiffest coordinate) was observed for any value of Δt . These results are consistent with the finding of Helfand et al.²⁶ that the stretching coordinate has very little effect on the rate of conformational transitions in polyethylene.

No significant temperature dependence was noted in the coupling of various degrees of freedom to the transforming bond except for bond angle coupling. As Δt was increased, the magnitude of the bond angle distortion decreased more slowly at low temperatures.

Experimental Estimates of the Length Scale of Cooperativity. As shown above, simulations of polyisoprene

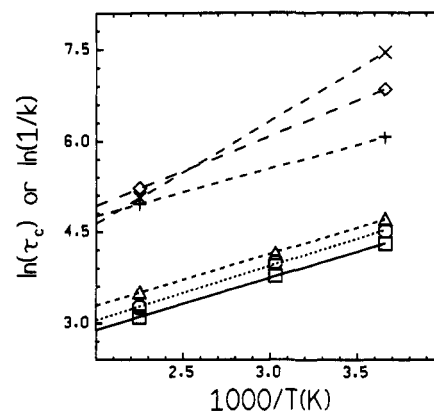


Figure 7. Comparison of transition rates (k) for conformational transitions and P_2 correlation times (τ_c) for reorientation of C-H vectors. Correlation times are represented by carbon a (\square), carbon b (\circ), and carbon c (Δ). Transition rates are represented by $\alpha\gamma$ (+), $\gamma\beta$ (\diamond), and $\beta\alpha$ (\times). Both correlation times and inverse rates are given in units of picoseconds. Estimated errors in both quantities are 10%.

indicate that a conformational transition requires cooperative motion of the neighboring one to two repeat units. This is roughly consistent with inferences drawn from recent experimental work on polyisoprene. Adachi and Kotaka have conducted dielectric relaxation studies of polyisoprene in solution and in the bulk.²⁷ Using the Rouse theory to interpret their results, they estimated that the fundamental unit for segmental motions was one to three repeat units, depending upon the solution concentration. Hyde and Ediger recently studied the reorientation of rigid probe molecules in bulk polyisoprene over a wide temperature range.²⁸ They found that motions on the scale of 8–12 Å have the same temperature dependence as large-scale chain motions. A reasonable interpretation of this result would be that 8–12 Å (two to three repeat units) is an upper bound on the fundamental unit for segmental motion.

Transition Rates vs Correlation Times. Given a definition of a conformational transition, transition rates may be directly determined from the simulation trajectory. The inverses of the temperature-dependent transition rates for each of the three types of backbone bonds are shown in the top part of Figure 7. Shown near the bottom are the P_2 correlation times for three different C-H vectors within the repeat unit. As expected, the inverses of the transition rates are significantly slower than the correlation times; the P_2 correlation times qualitatively represent motion through an angle of about 45°, while transitions correspond to motion of 120° or 180°.

It is apparent from Figure 7 that the transition rates for the three types of backbone bonds do not have the same temperature dependence.²⁹ This is somewhat surprising considering that correlation times for the three different C-H vectors within the repeat unit all have the same temperature dependence. It is not clear whether the similar temperature dependence between one of the transition rates and the correlation times is coincidental or causal. Further studies with different potentials would be required to address this point.

Experimentalists often assume that correlation times are proportional to the inverse of conformational transition rates. Figure 7 indicates the possibility that this may not be true, depending upon which transition rate is of interest. For these simulations of polyisoprene, the correlation times have a different activation energy than the overall transition rate (7.6 vs 9.9 kJ/mol).

VI. Summary

A major emphasis of this paper has been to compare and to contrast our simulations with experimental observations. The encouraging agreement with NMR argues that the simulated dynamics are at least a fair representation of the actual dynamics of this system. The simulations indicate the presence of substantial librational motions on a time scale of a few picoseconds or less. For polyisoprene, distortions in atomic positions accompanying a conformational transition are localized to about one repeat unit. First-neighbor torsions play an important role in localizing transitions in polyisoprene but not in polyethylene.

Systematic improvements in the simulation should yield correspondingly better agreement with experimental results. This process of refinement may in itself provide insights into the fundamental origins of various features of local polymer motions. The treatment of solvent/polymer interactions with uncorrelated stochastic forces is one approximation that needs to be improved upon for the polyisoprene system. This approximation may be adequate for modeling polymers with bulky side groups where a linear scaling of τ_C with viscosity is observed. With increased computational capabilities, it may be possible to perform a molecular dynamics simulation on the polyisoprene system. Such a simulation might improve the agreement with experiments in several respects. Future simulations will be able to utilize the techniques we have developed to examine microscopic features of the local dynamics.

The systematic simulation of the local dynamics of a variety of polymers promises to enhance our understanding of structure/property relationships. It will be particularly interesting to compare the length scales associated with conformation transitions in different polymers. This length scale may correlate with the glass transition temperature of the polymers.

Acknowledgment. This work was supported by the National Science Foundation (DMR-8822076). We gratefully acknowledge helpful discussions with Eugene Helfand, Alan English, and Radley Olson. D.B.A. is grateful for fellowship support from the American Chemical Society. M.D.E. thanks the Alfred P. Sloan Foundation for a research fellowship. We also acknowledge a generous grant of computing time from IBM which made this work possible.

References and Notes

- (1) See, for example: (a) Ediger, M. D. *Annu. Rev. Phys. Chem.*, in press. (b) Heatley, F. *Annu. Rep. NMR Spectrosc.* **1986**, *17*, 179 and references therein.

- (2) (a) Helfand, E.; Wasserman, Z. R.; Weber, T. A. *Macromolecules* **1980**, *13*, 526. (b) Weber, T. A.; Helfand, E. A. *J. Phys. Chem.* **1983**, *87*, 2881.
- (3) van Gunsteren, W. F.; Berendsen, H. J. C. *Angew. Chem. Int. Ed. Engl.* **1990**, *29*, 992.
- (4) Levy, R. M.; Karplus, M.; McCammon, J. A. *Chem. Phys. Lett.* **1979**, *65*, 1538.
- (5) Brown, M. S.; Grant, D. M.; Horton, W. J.; Mayne, C. L.; Evans, G. T. *J. Am. Chem. Soc.* **1985**, *107*, 6698.
- (6) Fixman, M. J. *J. Chem. Phys.* **1978**, *68*, 1527, *J. Chem. Phys.* **1978**, *68*, 1538.
- (7) Adolf, D. B.; Ediger, M. D. *Computer Simulation of Polymers*; Prentice-Hall: Englewood Cliffs, NJ, 1991.
- (8) Three fictitious beads are placed on either end of the 201-bead polymer chain. This allows every bead within the chain to have potential contributions from two bond stretching interactions, three bond angle flexing interactions, and four dihedral angle interactions. The dynamics of the fictitious particles track those of the simulated particle removed 201 beads along the contour.
- (9) Edward, J. T. *J. Chem. Educ.* **1970**, *47*, 261.
- (10) Allinger, N. L. *J. Am. Chem. Soc.* **1977**, *99*, 8127.
- (11) (a) Helfand, E. *Bell Syst. Tech. J.* **1979**, *58*, 2289. (b) Green-side, H. S.; Helfand, E. A. *Bell Syst. Tech. J.* **1981**, *60*, 1927.
- (12) Glowinkowski, S.; Gisser, D. J.; Ediger, M. D. *Macromolecules* **1990**, *23*, 3520.
- (13) Gisser, D. J.; Glowinkowski, S.; Ediger, M. D. *Macromolecules* **1991**, *24*, 4270.
- (14) As discussed in refs 7 and 12, there are some very slow, very small amplitude components in the experimental correlation functions. These components are not included in the correlation time extracted from eq 8. These components are also excluded from the simulated correlation functions because of the length of the trajectories.
- (15) Provencher, S. W.; Vogel, R. H. *Progress in Scientific Computing*; Birkhaeuser: Boston, 1983; Vol. 2.
- (16) Dejean de la Batie, R.; Laupretre, F.; Monnerie, L. *Macromolecules* **1989**, *22*, 122.
- (17) Denault, J.; Prud'homme, J. *Macromolecules* **1989**, *22*, 1307.
- (18) Bagchi, G.; Oxtoby, D. W. *J. Chem. Phys.* **1983**, *78*, 2735.
- (19) Paul, E.; Mazo, R. M. *J. Chem. Phys.* **1968**, *48*, 1405.
- (20) Hall, C. K.; Helfand, E. *J. Chem. Phys.* **1982**, *77*, 3275.
- (21) Ferry, J. D. *Viscoelastic Properties of Polymers*; Wiley-Interscience: New York, 1980.
- (22) Grote, R. F.; Hynes, J. T. *J. Chem. Phys.* **1980**, *73*, 2715.
- (23) Helfand, E. *J. Chem. Phys.* **1971**, *54*, 4651; *Science* **1984**, *226*, 647.
- (24) Schatzki, T. F. *J. Polym. Sci.* **1962**, *57*, 496.
- (25) Adolf, D. B.; Ediger, M. D., submitted for publication in *Macromolecules*.
- (26) Helfand, E.; Wasserman, Z. R.; Weber, T. A.; Skolnick, J.; Runnels, J. H. *J. Chem. Phys.* **1981**, *75*, 4441.
- (27) Adachi, K.; Imanishi, Y.; Kotaka, T. *J. Chem. Soc., Faraday Trans. 1* **1989**, *85*, 1083.
- (28) Hyde, P. D.; Ediger, M. D. *J. Chem. Phys.* **1990**, *92*, 1036.
- (29) The definition of a transition is somewhat arbitrary.² We do not know whether other definitions would give qualitatively similar results.

Registry No. Polyisoprene, 9003-31-0.